

# Further numerical evidences for the gauge-independent separation between Confinement and Higgs phases in lattice $SU(2)$ gauge theory with a scalar field in the fundamental representation

Akihiro Shibata<sup>a,b,\*</sup> and Kei-Ichi Kondo<sup>c</sup>

<sup>a</sup>Computing Research Center, High Energy Accelerator Research Organization (KEK),  
Oho 1-1, Tsukuba 305-0801, Japan

<sup>b</sup>SOKENDAI (The Graduate University for Advanced Studies), Oho 1-1, Tsukuba 305-0801, Japan

<sup>c</sup>Department of Physics, Chiba University, 1-33 Yayoi-cho, Chiba 260, Japan

E-mail: <sup>a,b</sup>[akihiro.shibata@kek.jp](mailto:akihiro.shibata@kek.jp), <sup>c</sup>[kondok@faculty.chiba-u.jp](mailto:kondok@faculty.chiba-u.jp)

In the lattice gauge-scalar model with a single scalar field in the fundamental representation of the gauge group  $SU(2)$ , we have quite recently found that there exists a gauge-independent transition line separating the Confinement and Higgs phases without contradicting the well-known Osterwalder-Seiler-Fradkin-Shenker analyticity theorem between the two phases by performing numerical simulations without any gauge fixing. This was achieved by examining the correlation between the original fundamental scalar field and the so-called color-direction field constructed from the gauge field through the gauge-covariant decomposition due originally to Cho-Duan-Ge-Shabanov and Faddeev-Niemi.

In this presentation, we give further numerical evidence for the gauge-independent separation between the Confinement and Higgs phases in the above model to establish their physical origin. For this purpose, we investigate the separation line precisely. We also investigate the contributions of magnetic monopoles to examine their role in confinement from the viewpoint of the dual superconductor picture.

*The XVIth Quark Confinement and the Hadron Spectrum Conference (QCHSC24)*

*19-24 August, 2024*

*Cairns Convention Centre, Cairns, Queensland, Australia*

---

\*Speaker

## 1. Introduction

We investigate the gauge-scalar model on the lattice to clarify the mechanism of Confinement in the Yang-Mills theory in the presence of matter fields. We also investigate the non-perturbative characterization of the Brout-Englert-Higgs (BEH) mechanism [1], providing the gauge field with the mass in a gauge-independent way (without gauge fixing). However, it is impossible to realize the conventional BEH mechanism on the lattice unless the gauge fixing condition is imposed since gauge non-invariant operators have vanishing vacuum expectation value on the lattice without gauge fixing due to the Elitzur theorem [2]. This difficulty can be avoided by using the *gauge-independent description of the BEH mechanism* proposed recently by one of the authors, which needs neither the spontaneous breaking of gauge symmetry nor the non-vanishing vacuum expectation value of the scalar field [3, 4]. Therefore, we introduce the gauge-independent description of the BEH mechanism on the lattice and study the Higgs mechanism in a gauge-invariant way.

As for the gauge-scalar model with radially fixed scalar field (no Higgs mode) which transforms according to the *fundamental* representation of the gauge group  $SU(2)$ , we have quite recently found that there exists a gauge-independent transition line separating the Confinement and Higgs phases without contradicting the well-known Osterwalder-Seiler-Fradkin-Shenker analyticity theorem [5, 6] between the two phases by performing numerical simulations without any gauge fixing [7]. On the other hand, for the gauge-scalar model with a radially-fixed scalar field in the *adjoint* representation of the gauge group  $SU(2)$ , Brower et al. have shown that the Confinement and Higgs phases are completely separated into two different phases by a continuous transition line in the unitary gauge [8]. However, we have recently found a new transition line that divides completely the Confinement phase into two parts without gauge fixing [9].

This presentation gives further numerical evidence for the gauge-independent separation between the Confinement and Higgs phases in the above model to establish its physical origin. For this purpose, we accumulated the data for an extensive set of parameters  $(\beta, \gamma)$  using the method in [7, 9] with higher statistics. We further investigate the magnetic monopole in order to clarify the physical characteristics of each phase from the view of the dual superconductor picture.

## 2. $SU(2)$ lattice gauge-scalar model and gauge covariant decomposition

We introduce the lattice  $SU(2)$  gauge-scalar model with a single scalar field in the fundamental representation of the gauge group where the radial degrees of freedom of the scalar field is fixed (no Higgs modes) [7]. The action of this model with the gauge coupling constant  $\beta$  and the scalar coupling constant  $\gamma$  is given in the standard way by

$$S[U, \hat{\Theta}] = \frac{\beta}{2} \sum_{x, \mu > \nu} \text{Re tr} \left( \mathbf{1} - U_{x, \mu} U_{x+\hat{\mu}, \nu} U_{x+\hat{\nu}, \mu}^\dagger U_{x, \nu}^\dagger \right) + \frac{\gamma}{2} \sum_{x, \mu} \text{Re tr} \left( \mathbf{1} - \hat{\Theta}_x^\dagger U_{x, \mu} \hat{\Theta}_{x+\hat{\mu}} \right), \quad (1)$$

where  $U_{x, \mu} \in SU(2)$  is a (group-valued) gauge variable on a link  $\langle x, \mu \rangle$ , and  $\hat{\Theta}_x \in SU(2)$  is a (matrix-valued) scalar variable in the fundamental representation on a site  $x$  which obeys the unit-length (or radially fixed) condition:  $\hat{\Theta}_x^\dagger \hat{\Theta}_x = \mathbf{1} = \hat{\Theta}_x \hat{\Theta}_x^\dagger$ . This action is invariant under the local  $SU(2)_{\text{local}}$  gauge transformation and the global  $SU(2)_{\text{global}}$  transformation for the link variable  $U_{x, \mu}$  and the site variable  $\hat{\Theta}_x$ :  $U_{x, \mu} \mapsto U'_{x, \mu} = \Omega_x U_{x, \mu} \Omega_{x+\mu}^\dagger$  and  $\hat{\Theta}_x \mapsto \hat{\Theta}'_x = \Omega_x \hat{\Theta}_x \Gamma$  for  $\Omega_x \in SU(2)_{\text{local}}$ ,  $\Gamma \in SU(2)_{\text{global}}$ .

In our investigations, the color-direction field defined shortly plays the key role. This new field was introduced in the framework of change of field variables which is originally based on the gauge-covariant decomposition [10, 11] of the gauge field due to Cho-Duan-Ge-Shabanov[12–14] and Faddeev-Niemi[15]. (see [16] for a review.)

The *color-direction field* on the lattice is a (Lie-algebra valued) site variable:  $\mathbf{n}_x := n_x^A \sigma^A \in \text{su}(2) - \text{u}(1)$  ( $A = 1, 2, 3$ ) with the unit length  $\mathbf{n}_x \cdot \mathbf{n}_x = 1$ , where  $\sigma^A$  are the Pauli matrices. We require the transformation property of the color-direction field  $\mathbf{n}_x$  as  $\mathbf{n}_x \mapsto \mathbf{n}'_x = \Omega_x \mathbf{n}_x \Omega_x^\dagger$ .

For a given gauge field configuration  $\{U_{x,\mu}\}$ , we determine the color-direction field configuration  $\{\mathbf{n}_x\}$  (as the unique configuration up to the global color rotation) by minimizing the so-called *reduction functional*  $F_{\text{red}}[\mathbf{n}; U]$  under the gauge transformations:

$$F_{\text{red}}[\{\mathbf{n}\}; \{U\}] := \sum_{x,\mu} \frac{1}{4} \text{tr} \left[ (D_\mu[U] \mathbf{n}_x)^\dagger (D_\mu[U] \mathbf{n}_x) \right] = \sum_{x,\mu} \frac{1}{2} \text{tr} \left( \mathbf{1} - \mathbf{n}_x U_{x,\mu} \mathbf{n}_{x+\hat{\mu}} U_{x,\mu}^\dagger \right). \quad (2)$$

In this way, a set of color-direction field configurations  $\{\mathbf{n}_x\}$  is obtained as the (implicit) functional of the original link variables  $\{U_{x,\mu}\}$ , which is written symbolically as

$$\mathbf{n}^* = \underset{\mathbf{n}}{\text{argmin}} F_{\text{red}}[\{\mathbf{n}\}; \{U\}]. \quad (3)$$

This construction shows the nonlocal nature of the color-direction field.

By way of the color-direction field, the original link variable  $U_{x,\mu} \in \text{SU}(2)$  is gauge-covariantly decomposable into the product of two field variables  $X_{x,\mu}, V_{x,\mu} \in \text{SU}(2)$ :  $U_{x,\mu} = X_{x,\mu} V_{x,\mu}$ . We require that  $V_{x,\mu}$  has the transformation law in the same form as the original link variable  $U_{x,\mu}$  and that  $X_{x,\mu}$  has the transformation law in the same form as the site variable  $\mathbf{n}_x$ :

$$V_{x,\mu} \mapsto V'_{x,\mu} = \Omega_x V_{x,\mu} \Omega_{x+\hat{\mu}}^\dagger, \quad X_{x,\mu} \mapsto X'_{x,\mu} = \Omega_x X_{x,\mu} \Omega_x^\dagger. \quad (4)$$

This decomposition is uniquely determined by solving the *defining equations* simultaneously (once the color-direction field is given):

$$D_\mu[V] \mathbf{n}_x := V_{x,\mu} \mathbf{n}_{x+\hat{\mu}} - \mathbf{n}_x V_{x,\mu} = 0, \quad \text{tr}(\mathbf{n}_x X_{x,\mu}) = 0, \quad (5)$$

where  $D_\mu[V]$  denotes the covariant derivative in the adjoint representation. Indeed, the exact solution is obtained in the following form [11]:

$$V_{x,\mu} = \tilde{V}_{x,\mu} / \sqrt{\frac{1}{2} \text{tr}(\tilde{V}_{x,\mu}^\dagger \tilde{V}_{x,\mu})}, \quad \tilde{V}_{x,\mu} := U_{x,\mu} + \mathbf{n}_x U_{x,\mu} \mathbf{n}_{x+\hat{\mu}}, \quad X_{x,\mu} = U_{x,\mu} V_{x,\mu}^\dagger. \quad (6)$$

By introducing the color-direction field, we obtain the deformed theory in which the expectation value of an operator  $\mathcal{O}$  including the color-direction field is calculated according to

$$\langle \mathcal{O}[U, \hat{\Theta}, \mathbf{n}] \rangle = \frac{1}{Z} \int \mathcal{D}U \mathcal{D}\hat{\Theta} e^{-S[U, \hat{\Theta}]} \int \mathcal{D}\mathbf{n} \delta(\mathbf{n} - \mathbf{n}^*) \mathcal{O}[U, \hat{\Theta}, \mathbf{n}], \quad (7)$$

where  $\mathcal{D}\mathbf{n} = \prod_x d\mathbf{n}_x$  is the invariant measure for the color-direction field and  $\delta(\mathbf{n} - \mathbf{n}^*)$  is the Dirac delta function which plays the role of replacing  $\mathbf{n}$  by  $\mathbf{n}^*$  determined by (3).

It should be remarked that these new variables have been successfully used to understand confinement based on the dual superconductor picture. For example, it has been shown in the pure gauge theory without the matter field that the restricted field  $V$  gives the dominant part for quark confinement, while the remaining field  $X$  corresponds to the massive modes and decouples in the low-energy region. This gives the gauge-independent version of the Abelian dominance observed in the maximal Abelian gauge. See [16] for more details and more applications of this reformulation of the gauge theory.

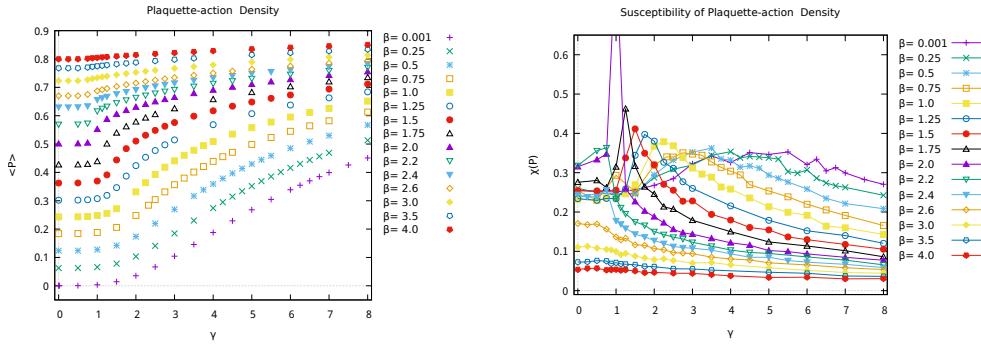


**Figure 1:** Left: Plots of  $\langle P \rangle$  for various  $\beta = \text{const.}$  Right: Plots of  $\chi(P)$  for various  $\beta = \text{const.}$  Lines in the plots are the eye guides for  $\beta = \text{const.}$

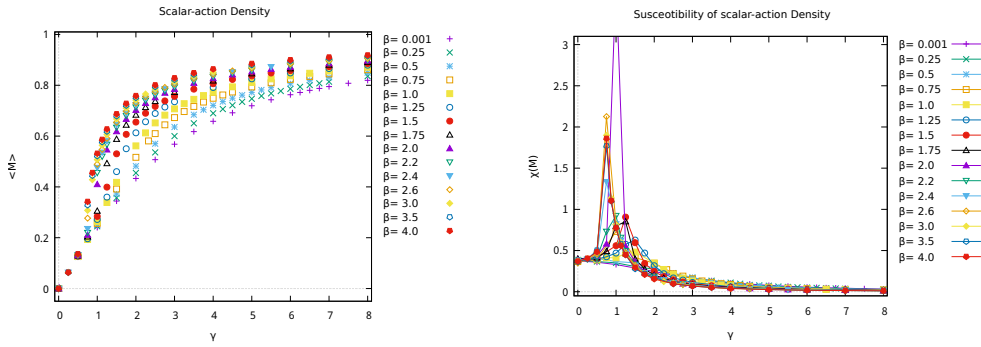


**Figure 2:** Left: Plots of  $\langle M \rangle$  for various  $\beta = \text{const.}$  Right: Plots of  $\chi(M)$  for various  $\beta = \text{const.}$

### 3. Lattice results

We perform the numerical simulation on the  $16^4$  lattice with the periodic boundary condition. Link variables  $\{U_{x,\mu}\}$  and scalar fields  $\{\Theta_x\}$  are updated alternately by using the HMC (Hamiltonian Monte Carlo) algorithm with integral interval  $\Delta\tau = 1$  without gauge fixing. After the thermalization of 5000 sweeps, we store 3000 configurations every five sweeps.

We search for a separation line that separates the phases or distinguishes the physical origin of confinement by measuring the expectation value  $\langle O \rangle$  of a chosen operator  $O$  by changing  $\gamma$  (or  $\beta$ ) along the  $\beta = \text{const.}$  (or  $\gamma = \text{const.}$ ) line. We identify the separation line by using singular property such as bends, steps, jumps, and gaps observed in the graph of the  $\langle O \rangle$  plots or peaks in the graph of susceptibility  $\chi(O)$  plots.

#### 3.1 Thermodynamic phase transition

We reexamine the separation line obtained from the action density with high statistics for an extensive set of parameter  $(\beta, \gamma)$  as in the previous work [7]:

$$P = \frac{1}{6N_{\text{site}}} \sum_x \sum_{\mu < \nu} \frac{1}{2} \text{tr} \left( U_{x,\mu} U_{x+\hat{\mu},\nu} U_{x+\hat{\nu},\mu}^\dagger U_{x,\nu}^\dagger \right), \quad \chi(P) = (6N_{\text{site}}) \{ \langle P^2 \rangle - \langle P \rangle^2 \}, \quad (8)$$

$$M = \frac{1}{4N_{\text{site}}} \sum_x \sum_{\mu} \frac{1}{2} \text{Retr} \left( \Theta_x^\dagger U_{x,\mu} \Theta_{x+\hat{\mu}} \right), \quad \chi(M) = (4N_{\text{site}}) \{ \langle M^2 \rangle - \langle M \rangle^2 \}, \quad (9)$$

where  $\langle O \rangle$  represents the average of the operator  $O$  over configurations. In this analysis, we focus on the susceptibility to determine the separation line.

Figure 1 shows the result of measurements for the plaquette density (8). The left panel shows the plot of  $\langle P \rangle$  for various  $\beta = \text{const.}$ , and the right panel shows the plot of the susceptibility  $\chi(P)$  for various  $\beta = \text{const.}$  There exist bends or gaps in the  $\langle P \rangle$  and peaks in the  $\chi(P)$  which correspond to the separation line. Note that there are two types of peaks for  $\chi(P)$ : a narrow and sharp peaks observed in  $\beta > \beta_c \simeq 0.75$ , and a broad and gradual peaks observed in  $\beta < \beta_c$ . In the same way, Fig.2 shows the result of measurements for the scalar density (9). The left panel shows the plot of  $\langle M \rangle$  for various  $\beta = \text{const.}$ , and the right panel the plot of susceptibility  $\chi(M)$  for various  $\beta = \text{const.}$

The left panel of Fig.4 shows the phase diagram determined from the action density. The dark blue plots represent the separation line determined from both the average of action densities,  $\langle P \rangle$ ,  $\langle M \rangle$ , and their susceptibilities,  $\chi(P)$ ,  $\chi(M)$ . This separation line could be the first order phase transition line and disappears in the region  $\beta < \beta_c$ , which is pointed out by the Osterwalder-Seiler-Fradkin-Shenker analyticity theorem [5, 6]. On the other hand, the orange plots in  $\beta < \beta_c$  represent the separation line suggested only by the susceptibility  $\chi(P)$ . This separation line could be the second order phase transition or the cross over. However, those peaks are not narrow and sharp but broad and gradual.

In addition, there exists the other separation line obtained only from  $\chi(P)$  (the orange plots in the region  $0 \leq \gamma < 1$  and  $2 < \beta < 2.5$ ) that separates between the scaling and non-scaling region, which corresponds to the "critical" point already discovered in the pure  $SU(2)$  Yang-Mills theory ( $\gamma = 0$ ) in [17, 18].

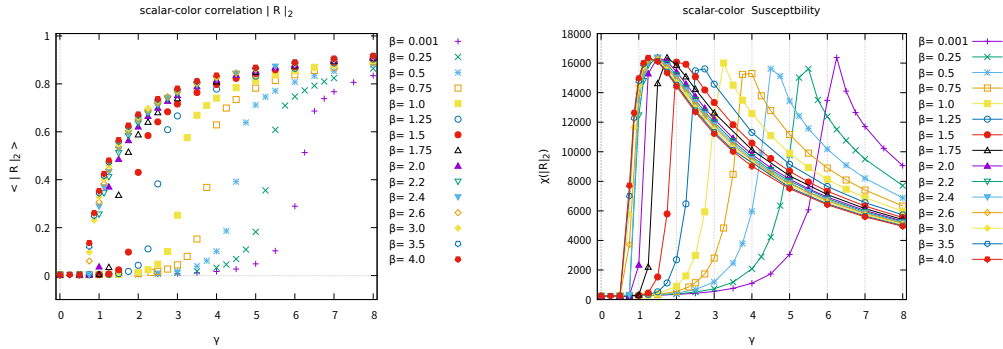


Figure 3: Left: Plots of  $\langle |R|_2 \rangle$  for various  $\beta = \text{const.}$  Right: Plots  $\chi(|R|_2)$  for various  $\beta = \text{const.}$

### 3.2 Scalar-color correlation

In order to reexamine the correlation between the scalar field and the color-direction field, as in the previous work [7]:

$$\mathbf{R} = \frac{1}{N_{\text{site}}} \sum_x \Theta_x^\dagger \mathbf{n}_x \Theta_x \quad \langle |R|_2 \rangle, \quad \chi(|R|_2) = (4N_{\text{site}}) \{ \langle |R|_2^2 \rangle - \langle |R|_2 \rangle^2 \}, \quad (10)$$

where  $|R|_2$  represents the 2-norm defined by  $|R|_2 = \sqrt{|R_1|^2 + |R_2|^2 + |R_3|^2}$  with  $R_A = \text{tr}(\mathbf{R}\sigma^A)$ .

The left panel of Fig.3 shows the plots of  $\langle |R|_2 \rangle$  v.s.  $\gamma$  for various  $\beta = \text{const.}$  We observe bends or gaps for all the  $\beta = \text{const.}$ , which correspond to the separation line. The right panel of Fig.3 shows the plots of the susceptibility  $\chi(|R|_2)$  v.s.  $\gamma$  for various  $\beta = \text{const.}$ , and we observe sharp peaks for all the  $\beta = \text{const.}$

The right panel of Fig.4 shows the separation line obtained from the scalar-color correlation. We determine the location of the phase separation line by using peaks of the susceptibility  $\chi(|\mathbf{R}|_2)$  plots rather than the bents or jumps in the  $\langle |\mathbf{R}|_2 \rangle$  plots, which causes its location to shift toward a larger  $\gamma$  compared to the previous work [7]. This suggest the separation between the Confinement and Higgs phases completely for all the region.

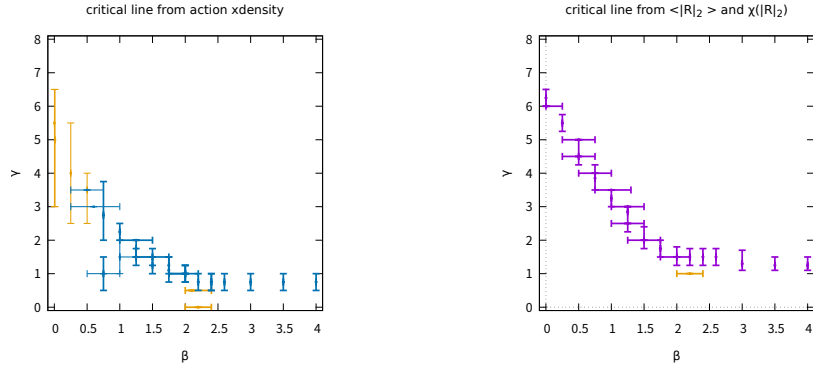


**Figure 4:** Left: The phase transition line determined from action density,  $\langle P \rangle$ ,  $\chi(P)$ ,  $\langle M \rangle$ , and  $\chi(M)$ . The orange plots represent that obtained only from  $\chi(P)$ . Right: The separation line determined from the scalar-color correlation  $\langle |\mathbf{R}|_2 \rangle$ ,  $\chi(|\mathbf{R}|_2)$ .

### 3.3 Contribution of the magnetic monopole

Moreover, we investigate the contribution of the magnetic monopole to clarify the physical origin of the separation of the Confinement and Higgs phases in view of the dual superconductor picture [19] where magnetic monopoles play the dominant role in confinement.

We can define the magnetic monopole,  $k_{x,\mu}$  in a gauge-independent (gauge-invariant) way through the gauge-covariant decomposition [16]:

$$F(x)_{\mu\nu} := \arg_F \text{tr} \left\{ (\mathbf{1} + \mathbf{n}_x) V_{x,\mu} V_{x+\hat{\mu},\nu} V_{x+\hat{\nu},\mu}^\dagger V_{x,\nu}^\dagger \right\},$$

$$k_{x,\mu} := \frac{1}{2} \epsilon^{\mu\nu\alpha\beta} (F(x+\hat{\nu})_{\alpha\beta} - F(x)_{\alpha\beta}) =: 2\pi m_{x,\mu}, \quad m_{x,\mu} = 0, \pm 1, \pm 2, \dots, \quad (11)$$

where  $V_{x,\mu}$  represents the restricted field obtained from the gauge-covariant decomposition (6), and  $\mathbf{n}_x$  the color-direction field determined by (3). This magnetic monopole takes the integer value and satisfies the current conservation law, i.e.,  $\partial_\mu k^{x,\mu} = \sum_\mu (k_{x+\hat{\mu},\mu} - k_{x,\mu}) = 0$ . Therefore, we define the magnetic-monopole-charge density:

$$\rho_k := \frac{1}{4N_{\text{site}}} \sum_{x,\mu} |m_{x,\mu}|. \quad (12)$$

Figure 5 shows the plot of the magnetic-monopole-charge density  $\langle \rho_k \rangle$ . The left panel shows the plot of  $\langle \rho_k \rangle$  along various  $\gamma = \text{const.}$  lines.  $\langle \rho_k \rangle$  decreases as  $\beta$  increases and there exist no singular points in the plots. Note that we observe very small  $\langle \rho_k \rangle$  for large  $\beta$ , which is measured not in the physical unit but in the lattice one. This is because the lattice spacing in the physical unit is a decreasing function of  $\beta$ , and for large  $\beta$  the physical volume becomes small against the lattice with fixed size.

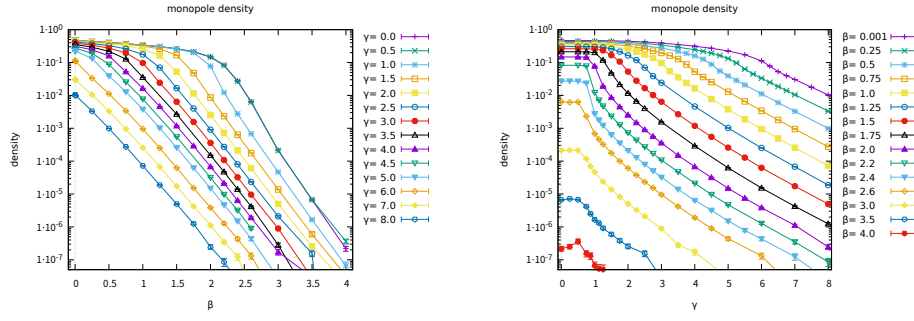


**Figure 5:** Left: Plots of  $\langle \rho_k \rangle$  v.s.  $\beta$  for various  $\gamma = \text{const.}$  Right: Plots of  $\langle \rho_k \rangle$  v.s.  $\gamma$  for various  $\beta = \text{const.}$  The lines in the plots are eye guide with  $\beta = \text{const.}$  or  $\gamma = \text{const.}$

The right panel of Fig.5 shows  $\langle \rho_k \rangle$  along various  $\beta = \text{const.}$  lines. In the region  $\gamma < \gamma_c(\beta)$ , where  $\gamma_c(\beta)$  represents the separation line in the right panel of Fig.4), the magnetic-monopoles-charge density  $\langle \rho_k \rangle$  is rich and constant along the  $\beta = \text{const.}$  line. It suggests that the magnetic monopole plays a dominant role in this region, which we call Confinement phase. In contrast, we observe less or vanishing magnetic monopoles in the region  $\gamma > \gamma_c(\beta)$ . In the region  $\beta > \beta_c \simeq 0.75$ , we observe bends or steps at  $\gamma$  being the phase separation line,  $\gamma = \gamma_c(\beta)$ , and the magnetic monopoles disappear for  $\gamma > \gamma_c(\beta)$ . Therefore, the gluons gain mass due to the BEH mechanism and are confined. We call this region the Higgs phase. While, in the region  $\beta < \beta_c$  there exist no more bends or steps for  $\langle \rho_k \rangle$ , and  $\langle \rho_k \rangle$  decreases rather smoothly as  $\gamma$  increase. The separation line  $\gamma_c(\beta)$  could not be a phase transition line but be the boundary where the two physical origins switch over continuously.

#### 4. Summary

We have reexamined the  $SU(2)$  gauge-scalar model with the scalar field in the fundamental representation to obtain further numerical evidence for the gauge-independent separation between the Confinement and Higgs phases based on the method in the previous work [7, 9]. We have confirmed the thermodynamic phase transition, which is consistent with the Osterwalder-Seiler-Fradkin-Shenker analyticity theorem. We have also reexamined the separation line that separates the Confinement and Higgs phases based on the covariant decomposition of the gauge field and confirmed it. Although it could not be the thermodynamic phase transition line, it could be the separation line that distinguishes the physical origin of the confinement.

Moreover, we have investigated the magnetic-monopole-charge density to clarify the physical origin of the separation line. We have confirmed that in the Confinement phase the magnetic monopole plays a dominant role in confinement, while in the Higgs phase the magnetic monopoles disappear and the Yang-Mills field acquires the mass through the BEH mechanism and is confined.

#### Acknowledgments

This work was supported by Grant-in-Aid for Scientific Research, JSPS KAKENHI Grant Number (C) No.23K03406. The numerical simulation was supported in part by the Multidisciplinary Cooperative Research Program in CCS, University of Tsukuba.

## References

- [1] P.W. Higgs, Phys. Lett. **12**, 132 (1964); Phys. Rev. Lett. **13**, 508 (1964).  
F. Englert and R. Brout, Phys. Rev. Lett. **13**, 321 (1964).
- [2] S. Elitzur, Phys. Rev. D **12**, 3978 (1975).
- [3] K.-I. Kondo, Phys. Lett. B **762**, 219 (2016). arXiv:1606.06194 [hep-th]
- [4] K.-I. Kondo, Eur. Phys. J. C **78**, 577 (2018). arXiv:1804.03279 [hep-th]
- [5] K. Osterwalder and E. Seiler, Annls. Phys **110**, 440 (1978).
- [6] E. Fradkin and S.H. Shenker, Phys. Rev. D **19**, 3682 (1979).
- [7] R. Ikeda, S. Kato, K.-I. Kondo, and A. Shibata, Phys. Rev. D **109**, 054505 (2024),  
arXiv:2308.13430, CHIBA-EP-259/KEK Preprint 2023-27
- [8] R.C. Brower, D.A. Kessler, T. Schalk, H. Levine, and M. Nauenberg, Phys. Rev. D **25**, 3319 (1982).
- [9] A. Shibata and K.-I. Kondo, Phys. Rev. D **110**, 3, 034508 (2024), arXiv:2307.15953 [hep-lat],  
KEK Preprint 2023-24/CHIBA-EP-258
- [10] A. Shibata, S. Kato, K.-I. Kondo, T. Murakami, T. Shinohara, and S. Ito, Phys. Lett. B **653**,  
101(2007). arXiv:0706.2529 [hep-lat]
- [11] A. Shibata, K.-I. Kondo, and T. Shinohara, Phys. Lett. B **691**, 91 (2010). arXiv:0706.2529 [hep-lat]
- [12] Y.M. Cho, Phys. Rev. D **21**, 1080 (1980); Phys. Rev. D **23**, 2415 (1981).
- [13] Y.S. Duan and M.L. Ge, Sinica Sci. **11**, 1072 (1979).
- [14] S.V. Shabanov, Phys. Lett. B **463**, 263 (1999). [hep-th/9907182]
- [15] L.D. Faddeev and A.J. Niemi, Phys. Rev. Lett. **82**, 1624 (1999). [hep-th/9807069];  
L.D. Faddeev and A.J. Niemi, Nucl. Phys. B **776**, 38 (2007). [hep-th/0608111]
- [16] K.-I. Kondo, S. Kato, A. Shibata, and T. Shinohara, Phys. Rept. **579**, 1–226 (2015).  
arXiv:1409.1599 [hep-th]
- [17] G. Bhanot and M. Creutz, Phys. Rev. D **24**, 3212 (1981).
- [18] M. Creutz, *Quarks, Gluons and Lattices*, Cambridge Monographs on Mathematical Physics  
(Cambridge University Press, 1985).
- [19] Y. Nambu, Phys. Rev. D **10**, 4262 (1974).  
G. 't Hooft, in *High Energy Physics*, edited by A. Zichichi (Editorice Compositori, Bologna,  
1975).  
S. Mandelstam, Phys. Rep. **23**, 245 (1976).